Output Feedback Control of Parabolic PDE Systems with Nonlinear Spatial Differential Operators

James Baker and Panagiotis D. Christofides*

Department of Chemical Engineering, University of California, Los Angeles, California 90095-1592

This article focuses on nonlinear static (direct) output feedback control of parabolic partial differential equations (PDE) systems with nonlinear spatial differential operators with application to a rapid thermal chemical vapor deposition (RTCVD) process. Initially, a detailed mathematical model is presented for the RTCVD process, which consists of a nonlinear parabolic PDE that describes the spatiotemporal evolution of the wafer temperature, coupled with a set of nonlinear ordinary differential equations (ODEs) that describes the time evolution of the chamber temperature and the concentrations of the various species. Then, a systematic methodology is presented for the synthesis of nonlinear static output feedback controllers for parabolic PDE systems with nonlinear spatial differential operators. Initially, the Karhunen−Loéve expansion is used to derive empirical eigenfunctions of the nonlinear parabolic PDE system, then the empirical eigenfunctions are used as basis functions within a Galerkin model reduction framework to derive low-order ODE systems that accurately describe the dominant dynamics of the PDE system, and finally, these ODE systems are used for the synthesis of nonlinear static output feedback controllers that guarantee stability and enforce output tracking in the closed-loop system. The proposed control method is employed to synthesize a nonlinear easy-to-implement controller for the RTCVD process that uses measurements of wafer temperature at five locations to manipulate the power of the top lamps in order to achieve uniform temperature and, thus, uniform deposition of a thin film on the wafer over the entire process cycle. The performance of the developed nonlinear output feedback controller is successfully tested through simulations and is shown to be superior to the one of a linear control scheme.

Introduction

Rapid thermal chemical vapor deposition (RTCVD) is a rapidly growing technology in the microelectronics industry. The central idea of RTCVD is to use a series of lamps to radiatively heat a wafer from room temperature to 1200 K at very high heating rates (more than 150 K/s), and then keep it at the high temperature for a short time. This sharp increase in the temperature of the wafer reduces significantly the overall thermal budget of the process (the overall processing time is usually less than 1 min) and the diffusion length, thereby preserving dopant profiles from previous steps, and allows the fabrication of very small devices by using temperature as a switch in ending a process cycle. These features make RTCVD an attractive alternative over conventional furnace-based chemical vapor deposition processes employed in the fabrication of devices with submicrometer dimensional constraints. Even though RTCVD possesses many significant advantages, its widespread use is seriously limited by the lack of adequate wafer temperature control to achieve the tight requirements of uniformity and repeatability set by the industry. The main obstacles in achieving spatially uniform wafer temperature (and thus, uniform film deposition) are the highly nonlinear, time-varying and spatially varying nature of the RTCVD process that makes the development and implementation of effective model-based feedback controllers a very difficult task (e.g. refs 4, 5, 17, and 21). The main challenge in the design of model-based feedback controllers for RTCVD processes is that the dynamic models of such processes consist of nonlinear parabolic partial differential equation (PDE) systems, which are distributed parameter (infinite-dimensional) systems, and thus, they cannot be directly used for the design of practically implementable (low-dimensional) controllers.

Even though nonlinear parabolic PDE systems are infinite dimensional in nature, their dominant dynamic behavior is usually characterized by a finite (typically small) number of degrees of freedom. This implies that the dynamic behavior of such systems can be approximately described by ordinary differential equation (ODE) systems. Therefore, the standard approach to the control of linear/quasi-linear parabolic PDE systems involves the application of Galerkin's method (where the basis functions used to expand the solution of the system are typically the eigenfunctions of the spatial differential operator) to the PDE system to derive ODE systems that accurately describe the dynamics of the dominant (slow) modes of the PDE system. These ODE systems are subsequently used as the basis for controller synthesis (see, for example, refs 1 and 16). The main disadvantage of this approach is that the number of modes that should be retained to derive an ODE system that yields the desired degree of approximation may be very large, leading to complex controller design and high dimensionality of the resulting controllers. A natural approach to the construction of low-dimensional ODE systems that accurately reproduce the dynamics and solutions of quasi-linear parabolic PDE systems is based on the concept of approximate inertial manifold (see, for example, refs 8, 9, and 22 and the references therein).

* Author to whom correspondence should be addressed: (e-mail) pdc@seas.ucla.edu.

10.1021/ie990131c CCC: $18.00
Published on Web 10/08/1999

This concept was used in ref 7 for the construction of low-order controllers for parabolic PDE systems.

In the case of parabolic PDE systems with nonlinear spatial differential operators, as the ones that arise in the modeling of RTCVD processes, the selection of an appropriate basis to expand the solution of the PDE system is not an easy task because the eigenvalue problem cannot be solved analytically. An approach to address this problem is to utilize detailed finite difference (element) simulations of the PDE system to compute a set of *empirical eigenfunctions* (dominant spatial patterns) of the system through Karhunen−Loéve (K−L) decomposition (also known as proper orthogonal decomposition and principal component analysis). The use of empirical eigenfunctions as basis functions in Galerkin's method has been shown to lead to the derivation of accurate nonlinear low-dimensional approximations of several dissipative PDE systems arising in the modeling of diffusion−reaction processes and fluid flows (e.g., refs 2, 3, 15, and 23). Recently, linear feedback controllers were synthesized[18,24] for specific diffusion−reaction systems on the basis of low-dimensional models obtained by using empirical eigenfunctions as basis functions in Galerkin's method.

This work focuses on nonlinear static (direct) output feedback control of parabolic PDE systems with nonlinear spatial differential operators with application to an RTCVD process. Initially, a detailed mathematical model is presented for a low-pressure RTCVD process consisting of a nonlinear parabolic PDE that describes the spatiotemporal evolution of the wafer temperature, coupled with a set of nonlinear ODEs that describes the time evolution of the chamber temperature and concentrations of the various species. Then, a systematic methodology is presented for the synthesis of nonlinear static output feedback controllers for parabolic PDE systems with nonlinear spatial differential operators. Initially, the Karhunen−Loéve expansion is used to derive empirical eigenfunctions of the nonlinear parabolic PDE system, then the empirical eigenfunctions are used as basis functions within a Galerkin's model reduction framework to derive low-order ODE systems that accurately describe the dominant dynamics of the PDE system, and finally, these ODE systems are used for the synthesis of nonlinear static output feedback controllers that guarantee stability and enforce output tracking in the closed-loop system. The proposed control method is employed to synthesize a nonlinear easy-to-implement controller for the RTCVD process that uses measurements of wafer temperature at five locations to manipulate the power of the top lamps in order to achieve uniform temperature and, thus, uniform deposition of a thin film on the wafer over the entire process cycle. The performance of the developed nonlinear output feedback controller is successfully tested through simulations and is shown to be superior to the one of a linear control scheme.

Rapid Thermal Chemical Vapor Deposition: Description and Modeling

We consider a low-pressure RTCVD process shown in Figure 1; all the details on the description and modeling of the process can be found in ref 23. Here, we limit our discussion to the essential features of the process and the basic equations of the process model. Specifically, the process consists of a quartz chamber, three banks of tungsten heating lamps that are used to heat the wafer and a fan, which is located at the bottom of the reactor and is used to cool the chamber. The furnace is designed so that the top lamp bank A and the bottom lamp bank C heat the total area of the wafer, while the lamp bank B, which surrounds the reactor, is used to heat the wafer edge in order to compensate for heat loss that occurs from the edge (radiative cooling between wafer edge and quartz chamber). The wafer is rotated while heated for azimuthal temperature uniformity. The objective of the process is to deposit a 0.5-μm film of polycrystalline silicon on a 6-in. wafer in 40 s by feeding the reactor (from a small opening on the top) with 10% SiH_4 in Ar at 5 Torr pressure and using the heating lamps to heat the wafer from room temperature to 1200 K (this is the temperature where the deposition reactions take place), at a heating rate of the order of 180 K/s.

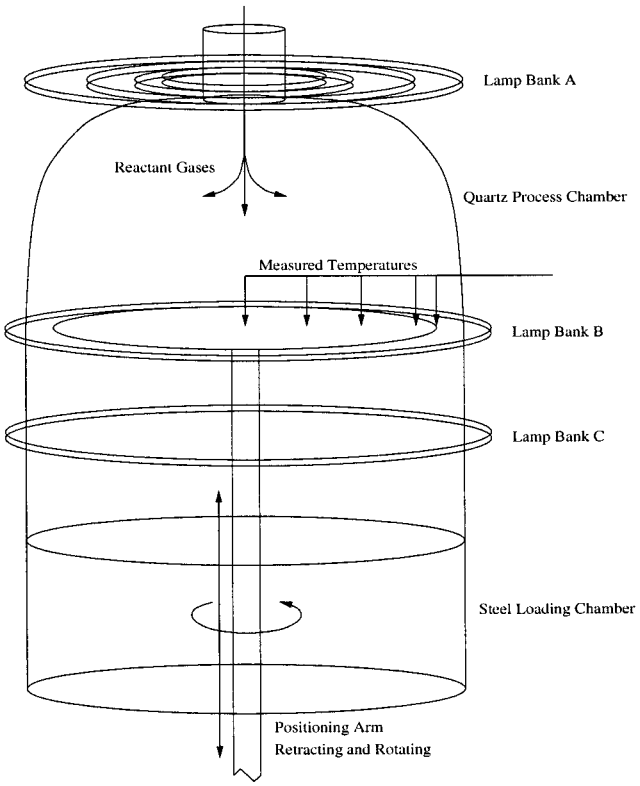

Figure 1. Rapid thermal chemical vapor deposition process: control configuration.

Under standard modeling assumptions, an energy balance on the wafer yields the following nonlinear parabolic PDE:

$$\rho_w T_{amb} \frac{\partial}{\partial t}(C_{p_w}(T)T) = \frac{T_{amb}}{R_w^2}\frac{1}{r}\frac{\partial}{\partial r}\left(\kappa(T) r \frac{\partial T}{\partial r}\right) - \frac{q_{rad}(T,r)}{\partial z} \quad (1)$$

subject to the boundary conditions

$$\left.\frac{\partial T}{\partial r}\right|_{r=0} = 0 \quad (2)$$

$$\left.\left(\kappa(T)\frac{\partial T}{\partial r}\right)\right|_{r=1} = -\sigma\epsilon_w T_{amb}^4(T^4 - T_c^4) + q_{edge}u_b \quad (3)$$

In the above equations, T_{amb} denotes the ambient temperature, $T = T'/T_{amb}$ denotes the dimensionless

wafer temperature, ρ_w, C_{p_w}, and R_w denote the density, heat capacity, and radius of the wafer, respectively, $r = r'/R_w$ denotes the dimensionless radial coordinate, q_{rad} is a term that accounts for radiative energy transfer between the wafer and its environment, $T_c = T_c'$ denotes the dimensionless temperature of the chamber, α denotes the Boltzmann constant, ϵ_ω denotes the emissivity of the wafer, q_{edge} denotes the energy flux at the edge of the wafer, and u_b denotes the percentage of the side lamp power that is used. The wafer heat capacity and thermal conductivity depend on temperature; their expressions and the expression of the radiative energy transfer terms q_{rad}, q_{edge} can be found in ref 23.

An energy balance on the quartz chamber yields the following ordinary differential equation.

$$T_{amb}M_c\frac{dT_c}{dt} = \epsilon_c Q_{lamps}u - A_{hem}q_h - A_{cyl}q_c - Q_{convect} - \sigma\epsilon_c A_c T_{amb}{}^4(T_c{}^4 - 1) \quad (4)$$

where M_c denotes the chamber thermal mass, ϵ_c denotes the emissivity of the chamber, A_{hem} denotes the chamber hemispherical area, A_{cyl} denotes the chamber cylindrical area, and A_c denotes the chamber outside area. q_h and q_c denote the net energy radiated from the hemispherical and cylindrical portions of the quartz chamber, respectively. The term $Q_{lamps}\,u$ represents energy absorbed by the chamber directly from the heating lamps, while $Q_{convect}$ denotes the energy transferred from the quartz chamber to the cooling gas by forced convective cooling. The explicit form of the terms in the right-hand side of eq 4 is given in ref 23.

The low-pressure conditions in the chamber allow us to assume perfect mixing of the reacting mixture, which, in turn, allows us to derive the following set of ODEs, which describe the time evolution of the molar fraction of SiH_4, X_{SiH_4}, and hydrogen, X_{H_2}:

$$\frac{dX_{SiH_4}}{dt} = -\alpha\int_{A_w} R_s(T,X_{SiH_4},X_{H_2})\,dA_w + \frac{1}{\tau}(X_{SiH_4}^{in} - X_{SiH_4})$$

$$\frac{dX_{H_2}}{dt} = 2\alpha\int_{A_w} R_s(T,X_{SiH_4},X_{H_2})\,dA_w - \frac{1}{\tau}X'_{H_2} \quad (5)$$

where α is the mole to mole conversion factor, A_w is the wafer area, τ is the residence time, $X_{SiH_4}^{in}$ is the molar fraction of SiH_4 in the inlet stream to the reactor and R_s is the rate of the deposition reactions:

$$R_s(T,X_{SiH_4},X_{H_2}) = \frac{k_0\exp\left(\frac{-\gamma}{RTT_{amb}}\right)X_{SiH_4}P_{tot}}{1 + bX_{SiH_4}P_{tot} + \frac{\sqrt{X_{H_2}P_{tot}}}{c}} \quad (6)$$

where k_0 is the pre-exponential constant, γ is the activation energy for deposition, P_{tot} is the total pressure, and b and c are constants. The deposition rate of Si onto the wafer surface is governed by the following expression:

$$\frac{dS}{dt} = \frac{MW_{Si}}{\rho_{Si}}R_s(T,X_{SiH_4},X_{H_2}) \quad (7)$$

where MW_{Si} and ρ_{Si} denote the molecular weight and density of Si, respectively. Referring to the expression of the deposition rate, we note the Arrhenius dependence of the deposition rate on wafer temperature, which clearly shows that nonuniform temperature results in nonuniform deposition, thereby implying the need to develop and implement a nonlinear feedback controller on the the process in order to achieve radially uniform wafer temperature. To this end, we present in the next section a general method for the synthesis of nonlinear static output feedback controllers for a class of nonlinear parabolic PDE systems that include the eq 1.

Static Output Control of Nonlinear Parabolic PDE Systems

(1) Description of Nonlinear Parabolic PDE Systems. We consider nonlinear parabolic PDE systems in one spatial dimension with the following state space description:

$$\partial\bar{x}/\partial t = L(\bar{x}) + wb(z)u + f(\bar{x})$$
$$y_c^i = \int_\alpha^\beta c^i(z)k\bar{x}\,dz, \quad i = 1, ..., l \quad (8)$$
$$y_m^\kappa = \int_\alpha^\beta s^\kappa(z)\omega\bar{x}\,dz, \quad \kappa = 1, ..., p$$

subject to the boundary conditions

$$C_1\bar{x}(\alpha,t) + D_1\frac{\partial\bar{x}}{\partial z}(\alpha,t) = R_1,$$
$$C_2\bar{x}(\beta,t) + D_2\frac{\partial\bar{x}}{\partial z}(\beta,t) = R_2 \quad (9)$$

and the initial condition

$$\bar{x}(z,0) = \bar{x}_0(z) \quad (10)$$

where $\bar{x}(z,t) = [\bar{x}_1(z,t)\cdots\bar{x}_n(z,t)]^T$ denotes the vector of state variables, $z \in [\alpha,\beta] \subset IR$ is the spatial coordinate, $t \in [0,\infty]$ is the time, $u = [u^1\ u^2\ \cdots\ u^l]^T \in IR^l$ denotes the vector of manipulated inputs, $y_c^i \in IR$ denotes the ith controlled output, and $y^\kappa{}_m \in IR$ denotes the κth measured output. $L(\bar{x})$ is a nonlinear differential operator that involves first- and second-order spatial derivatives, $f(\bar{x})$ is a nonlinear vector function, w, k, and ω are constant vectors, A, B, C_1, D_1, C_2, and D_2 are constant matrices, R_1 and R_2 are column vectors, and $\bar{x}_0(z)$ is the initial condition. $b(z)$ is a known smooth vector function of z of the form $b(z) = [b^1(z)\ b^2(z)\cdots b^l(z)]$, where $b^i(z)$ describes how the control action $u^i(t)$ is distributed in the interval $[\alpha,\beta]$, $c^i(z)$ is a known smooth function of z, which is determined by the desired performance specifications in $[\alpha,\beta]$, and s^κ is a known smooth function of z, which is determined by the location and "shape" of the measurement sensor (e.g., point/distributed sensing). Throughout the paper, we will use the order of magnitude notation $O(\epsilon)$. In particular, $\delta(\epsilon) = O(\epsilon)$ if there exist positive real numbers k_1 and k_2 such that $|\delta(\epsilon)| \le k_1|\epsilon|$, $\forall\ |\epsilon| < k_2$.

In order to simplify the presentation of the theoretical results of the paper, we formulate the parabolic PDE system of eq 8 as an infinite dimensional system in the Hilbert space $H([\alpha,\beta], IR^n)$ with H being the space of n-dimensional vector functions defined on $[\alpha,\beta]$ that satisfy the boundary condition of eq 9, with inner

product and norm $(\omega_1,\omega_2) = \int_\alpha^\beta (\omega_1(z),\omega_2(z))_{IR^n}\, dz$, $||\omega_1||_2 = (\omega_1,\omega_1)^{1/2}$, where ω_1,ω_2 are two elements of $H([\alpha,\beta];IR^n)$ and the notation $(\cdot,\cdot)_{IR^n}$ denotes the standard inner product in IR^n. Defining the state function x on $H([\alpha,\beta],IR^n)$ as $x(t) = \bar{x}(z,t)$, $t > 0$, $z \in [\alpha,\beta]$, the operator A in $H([\alpha,\beta],IR^n)$ as

$$A(x) = L(\bar{x}),\ x \in D(A) = \Big\{ x \in H([\alpha,\beta];\ IR^n);\ C_1\bar{x}(\alpha,t) + D_1\frac{\partial \bar{x}}{\partial z}(\alpha,t) = R_1;\ C_2\bar{x}(\beta,t) + D_2\frac{\partial \bar{x}}{\partial z}(\beta,t) = R_2 \Big\} \quad (11)$$

and the input and output operators as $Bu = wbu$, $Cx = (c, kx)$, and $Sx = (s, wx)$, where $c = [c^1\ c^2 \cdots c^l]$ and $s = [s^1\ s^2 \cdots s^p]$, the system of eqs 8−10 takes the form

$$\dot{x} = A(x) + Bu + f(x), \quad x(0) = x_0 \quad (12)$$

$$y_c = Cx, \quad y_m = Sx$$

where $f(x(t)) = f(\bar{x}(z,t))$ and $x_0 = \bar{x}_0(z)$. We assume that the nonlinear term $f(x)$ is locally Lipschitz with respect to its argument and satisfies $f(0) = 0$ and $\lim_{|x|\to 0}(|f(x)|/|x|) = 0$ (i.e., $f(x)$ does not include linear terms).

In the remainder of this section, we synthesize nonlinear static output feedback controllers for nonlinear parabolic PDE systems of the form of eq 8 by using the following approach: Initially, assuming that the solution of the parabolic PDE system of eq 8 is known, a set of empirical eigenfunctions (dominant spatial patterns) of the system will be computed using Karhunen−Loéve expansion. Then, the empirical eigenfunctions will be used as basis functions within a Galerkin model reduction framework to derive low-dimensional ODE systems that accurately reproduce the dynamics of the PDE system. Finally, these ODE systems will be used for the synthesis of nonlinear static output feedback controllers, which use on-line measurements of process outputs to stabilize the closed-loop system and force the outputs to follow their set-points.

(2) Karhunen−Loéve Expansion. In this section, we review the K−L expansion in the context of nonlinear one-dimensional parabolic PDE systems of the form of eq 8 with $n = 1$ (see refs 10 and 12 for a general presentation and analysis of the K−L expansion). We assume that the solution of the system of eq 8 is known and consider a sufficiently large set (which is called, ensemble), $\{\bar{v}_\kappa\}$, consisting of N sampled states, $\bar{v}_\kappa(z)$, (which are typically called "snapshots") of the solution of eq 8. To simplify our presentation, we assume uniform in time sampling of, $\bar{v}_\kappa(z)$, (i.e., the time interval between any two successive sampled states is the same), while we define the ensemble average of snapshots as $\langle\bar{v}_\kappa\rangle$: $= (1/K)\sum_{n=1}^K \bar{v}_n(z)$ (we note that nonuniform sampling of the snapshots and weighted ensemble average can be also considered; see, for example, ref 11). Furthermore, the ensemble average of snapshots $\langle\bar{v}_\kappa\rangle$ is subtracted out from the snapshots i.e.,

$$v_\kappa = \bar{v}_\kappa - \langle\bar{v}_\kappa\rangle \quad (13)$$

so that only fluctuations are analyzed. The problem is to compute the most characteristic structure $\phi(z)$ among these snapshots $\{v_\kappa\}$ that can be formulated as the one of maximizing the following objective function:

$$\text{maximize } \frac{\langle(\phi,v_\kappa)^2\rangle}{(\phi,\phi)}$$

$$s.t. (\phi,\phi) = 1, \quad \phi \in L^2([\alpha,\beta]) \quad (14)$$

The constraint $(\phi,\phi) = 1$ is imposed to ensure that the function, $\phi(z)$, computed as a solution of the above maximization problem, is unique. The Lagrangian functional corresponding to this constrained optimization problem is

$$\bar{L} = \langle(\phi,v_\kappa)^2\rangle - \lambda((\phi,\phi) - 1) \quad (15)$$

and necessary conditions for extremes is that the functional derivative vanishes for all variations $\phi + \delta\psi \in L^2[\alpha,\beta]$, where δ is a real number:

$$\frac{d\bar{L}(\phi + \delta\psi)}{d\delta}(\delta = 0) = 0, \quad (\phi,\phi) = 1 \quad (16)$$

Using the definitions of inner product and ensemble average, computing $d\bar{L}(\phi + \delta\psi)/d\delta)$ $(\delta = 0)$, and using that $\psi(\bar{z})$ is an arbitrary function, the following necessary conditions for optimality can be obtained:

$$\int_\alpha^\beta \langle v_\kappa(z)v_\kappa(\bar{z})\rangle\phi(z)\, dz = \lambda\phi(\bar{z}), \quad (\phi,\phi) = 1 \quad (17)$$

A computationally efficient way to obtain the solution of the above integral equation is provided by the method of snapshots,[19,20] where the requisite eigenfunction, $\phi(z)$, is expressed as a linear combination of the snapshots as follows:

$$\phi(z) = \sum_k c_k v_k(z) \quad (18)$$

Substituting the above expression for $\phi(z)$ on eq 17, we obtain the following eigenvalue problem

$$\int_\alpha^\beta \frac{1}{K}\sum_{\kappa=1}^K v_\kappa(z)v_\kappa(\bar{z})\sum_{k=1}^K c_k v_k(z)\, d\bar{z} = \lambda\sum_{k=1}^K c_k v_k(z) \quad (19)$$

Defining

$$B^{\kappa k} = \frac{1}{K}\int_\alpha^\beta v_\kappa(\bar{z})v_k(\bar{z})\, d\bar{z} \quad (20)$$

the eigenvalue problem of eq 19 can be equivalently written as

$$Bc = \lambda c \quad (21)$$

The solution of the above eigenvalue problem yields the eigenvectors $c = [c_1 \cdots c_K]$, which can be used in eq 18 to construct the eigenfunctions $\phi(z)$. From the structure of the matrix B, it follows that is symmetric and positive semidefinite, and thus, its eigenvalues, λ_κ, $\kappa = 1, \ldots, \kappa$, are real and non-negative. Furthermore, the computed eigenfunctions are orthogonal.

(3) Galerkin's Method. We derive an m-dimensional approximation of the system of eq 12 using Galerkin's method. Let H_s and H_f be two subspaces of H, defined as $H_s = \text{span}\{\phi_1, \phi_2, \ldots, \phi_m\}$ and $H_f = \text{span}\{\phi_{m+1}, \phi_{m+2}, \ldots\}$. The basis functions ϕ_j may be obtained through K−L expansion. Defining the orthogonal projection operators P_s and P_f such that $x_s = P_s x$, $x_f = P_f x$, the state x of the system of eq 12 can be decomposed as

$$x = x_s + x_f = P_s x + P_f x \tag{22}$$

Applying P_s and P_f to the system of eq l2 and using the above decomposition for x, the system of eq 12 can be equivalently written in the following form:

$$\begin{aligned} dx_s/dt &= A_s(x_s,x_f) + B_s u + f_s(x_s,x_f) \\ dx_f/dt &= A_f(x_s,x_f) + B_f u + f_f(x_s,x_f) \\ y_c &= Cx_s + Cx_f, \quad y_m = Sx_s + Sx_f \\ x_s(0) &= P_s x(0) = P_s x_0, \quad x_f(0) = P_f x(0) = P_f x_0 \end{aligned} \tag{23}$$

where $A_s(x_s,x_f) = P_s A(x_s + x_f)$, $B_s = P_s B$, $f_s = P_s f$, $A_f(x_s,x_f) = P_f A(x_s + x_f)$, $B_f = P_f B$, and $f_f = P_f f$. Owing to the parabolic nature of the spatial differential operator, the nonlinear vector $A_f(x_s,x_f)$ satisfies $A_f(x_s,x_f) = A_{fs}x_s + (1/\epsilon)A_f x_f + \bar{f}_f(x_s,x_f)$, where ϵ is a small positive parameter quantifying the separation between the slow (dominant) and fast (negligible) eigenmodes of the spatial operator, and A_{fs} and A_f are matrices with A_f being stable, and $\bar{f}_f(x_s,x_f)$ is a nonlinear vector function that does not include linear terms. Neglecting the infinite dimensional x_f subsystem in the system of eq 23 (this is equivalent to assuming that $\epsilon = 0$), the following m-dimensional slow system is obtained:

$$\begin{aligned} dx_s/dt = A_s(x_s) + B_s u + f_s(x_s,0) = \\ f_0(x_s) + \sum_{i=1}^{l} g_0^i u_0^i \\ y_{cs}{}^i = C^i x_s = h_0^i(x_s), \quad y_{ms} = Sx_s \end{aligned} \tag{24}$$

where the subscript s in $y_{cs}{}^i$ and y_{ms} is used to denote that these outputs are associated with a finite-dimensional system, the subscript 0 in (F_0, g_0^i, u_0^i, h_0^i) denotes that they are elements of the O(ϵ) approximation of the x_s subsystem of eq 23 (see proof of theorem 1 below for a precise characterization of the accuracy of the system of eq 14). We note that higher-order m-dimensional approximations of the system of eq 12 can be derived through combination of Galerkin's method with approximate inertial manifolds (see, for example, refs 6 and 7).

Remark 1. We note that when the approximate ODE model of eq 24 is obtained through Galerkin's method with empirical eigenfunctions, it provides a valid approximation of the parabolic PDE model in a broad region of the state space and not only in the region that was used for the computation of the snapshots, provided that the ensemble of snapshots is sufficiently large and contains sufficient information of the global dynamics of the PDE system. This property is a consequence of the fact that the empirical eigenfunctions form an orthogonal set of functions whose dimension is equal to the number of snapshots, and thus, it can be made arbitrarily large (even though completeness of this set cannot be guaranteed). Therefore, the use of empirical eigenfunctions for discretization of the PDE system is not fundamentally different from the use of other standard basis functions sets (sine and cosine functions, Legendre polynomials, etc.) for discretization with Galerkin's method, and thus, the finite-dimensional approximation obtained through Galerkin's method with empirical eigenfunctions is valid in a broad region of the state space. Such an ODE approximation, under standard smoothness assumptions of the solutions of the PDE, converges to the PDE system in an L^2 sense as the number of eigenfunctions used increases. Therefore, the ODE approximation of the PDE system obtained via Galerkin's method with empirical eigenfunctions is independent of the selection of the snapshots, as long as the dimension of this set is sufficiently large. Finally, the major practical benefit of using empirical eigenfunctions is that they directly satisfy the boundary conditions of the PDE system, a very important property for the case of PDEs with nonlinear boundary conditions (see, for example, the RTCVD process considered in the section on Nonlinear Static Output Feedback Control of RTCVD).

(4) Static Output Feedback Controller Design. We consider the synthesis of static output feedback control laws of the form

$$u_0 = p_0(y_m) + Q_0(y_m)\bar{v} \tag{25}$$

where $p_0(y_m)$ is a vector function, $Q_0(y_m)$ is a matrix, and $\bar{v}$ is a vector of the form $\bar{v} = V(v_i, v_i^{(1)},...,v_i^{(r_i)})$ where $V(v_i, v_i^{(1)},...,v_i^{(r_i)})$ is a smooth vector function, $v_i^{(k)}$ is the kth time derivative of the external reference input v_i (which is assumed to be a smooth function of time), and r_i is a positive integer.

The controller is constructed through combination of a state feedback controller design method and a procedure for the computation of estimates of x_s from the measurements y_m. Specifically, under the assumption that x_s is known, the computation of the explicit form of the functions $p_0(y_m)$, $Q_0(y_m)\bar{v}$ in the control law of eq 25 to enforce stability and output tracking in the closed-loop system will be done by utilizing standard geometric control methods for nonlinear ODEs.[13] Then, the following assumption is needed in order to obtain estimates of the states x_s of the system of eq 24 from the measurements y_m^κ, $\kappa = 1, ..., p$.

Assumption 1. $p = m$ (i.e., the number of measurements is equal to the number of slow modes), and the inverse of the operator S exists so that $\hat{x}_s = S^{-1}y_m$, where $\hat{x}_s$ is an estimate of x_s.

Note that the existence of the inverse of the matrix S depends on the location and shape (form of function s^κ) of the measurement sensors, and thus, s^κ should be properly chosen to ensure that S^{-1} exists. Theorem 1 below provides the synthesis formula of the output feedback controller and conditions that guarantee closed-loop stability. In order to state the theorem, we define for the system of eq 24 the relative order of the output y_{cs}^i with respect to the vector of manipulated inputs u as the smallest integer r_i for which

$$[L_{g_0^1} L_{f_0}^{r_i-1} h_0^i(x_s) \cdots L_{g_0^l} L_{f_0}^{r_i-1} h_0^i(x_s)] \not\equiv [0 \cdots 0] \tag{26}$$

or $r_i = \infty$ if such an integer does not exist, and the characteristic matrix

$$C_0(x_s) = \begin{bmatrix} L_{g_0^1} L_{f_0}^{r_1-1} h_0^1(x_s) & \cdots & L_{g_0^l} L_{f_0}^{r_1-1} h_0^1(x_s) \\ L_{g_0^1} L_{f_0}^{r_2-1} h_0^2(x_s) & \cdots & L_{g_0^l} L_{f_0}^{r_2-1} h_0^2(x_s) \\ \vdots & & \vdots \\ L_{g_0^1} L_{f_0}^{r_l-1} h_0^l(x_s) & \cdots & L_{g_0^l} L_{f_0}^{r_l-1} h_0^l(x_s) \end{bmatrix} \tag{27}$$

Theorem 1. Consider the parabolic PDE system of eq 12 and assume that assumption 1 holds. Consider also the ODE system of eq 24 and suppose that the following conditions hold: (1) The roots of the equation $\det(B(s)) = 0$, where $B(s)$ is a $l \times l$ matrix, whose (i, j)th element is of the form $\sum_{k=0}^{r_i} \beta_{jk}^i s^k$, lie in the open left half of the complex plane, and (2) the unforced ($v \equiv 0$) zero dynamics of the system of eq 24 is locally exponentially stable. Then, there exist constants μ_1, μ_2, and ϵ^* such that if $|x_s(0)| \le \mu_1, ||x_f(0)||_2 \le \mu_2$ and $\epsilon \in (0,\epsilon^*)$, then the static output feedback controller

$$u_0 = a_0(x_s,x_f,\bar{v},t) = \{[\beta_{1r_1} \cdots \beta_{lr_l}]C_0(y_m)\}^{-1}\{v - \sum_{i=1}^{l}\sum_{k=0}^{r_i}\beta_{ik}L_{f_0}^k h_0^i(y_m)\} \quad (28)$$

(a) guarantees exponential stability of the closed-loop system, and (b) ensures that the outputs of the closed-loop system satisfy for all $t \in [t_b,\infty)$:

$$y_c^i(t) = y_{cs}^i(t) + O(\epsilon), \quad i = 1, ..., l \quad (29)$$

where t_b is the time required for the off-manifold fast transients to decay to zero exponentially, and $y_{cs}^i(t)$ is the solution of

$$\sum_{i=1}^{l}\sum_{k=0}^{r_i}\beta_{ik}\frac{d^k y_{cs}^i}{dt^k} = v, \quad i = 1, ... l \quad (30)$$

Proof of Theorem 1. Substituting the controller of eq 28 into the parabolic PDE system of eq 12, we obtain

$$\dot{x} = Ax + Ba_0(x_s,x_f,\bar{v},t) + f(x), \quad x(0) = x_0$$
$$y_c = Cx, \quad y_m = Sx \quad (31)$$

A direct application of Galerkin's method to the above system with $H_s = \text{span}\{\phi_1,\phi_2,...,\phi_m\}$ and $H_f = \text{span}\{\phi_{m+1},\phi_{m+2},...\}$, and P_s and P_f such that $x_s = P_s x, x_f = P_f x$, yields

$$dx_s/dt = A_s(x_s,x_f) + B_s a_0(x_s,x_f,\bar{v},t) + f_s(x_s,x_f)$$
$$dx_f/dt = A_f(x_s,x_f) + B_f a_0(x_s,x_f,\bar{v},t) + f_f(x_s,x_f) \quad (32)$$

or

$$dx_s/dt = A_s(x_s,x_f) + B_s a_0(x_s,x_f,\bar{v},t) + f_s(x_s,x_f)$$
$$\epsilon\, dx_f/dt = \epsilon A_{fs}x_s,x_f + A_f x_f + \epsilon\bar{f}_f(x_s,x_f) + \epsilon B_f a_0(x_s,x_f,\bar{v},t) + \epsilon f_f(x_s,x_f) \quad (33)$$

The system of eq 33 is in the standard singularly perturbed form (see ref l4 for a precise definition of standard form), with x_s being the slow states and x_f being the fast states. Introducing the fast time scale $\tilde{\tau} = t/\epsilon$ and setting $\epsilon = 0$, we obtain the following infinite-dimensional fast subsystem from the system of eq 33:

$$dx_f/d\tilde{\tau} = A_f x_f \quad (34)$$

Since A_f is a stable matrix, we have that the above system is globally exponentially stable. Setting $\epsilon = 0$ in the system of eq 33, we have that $x_f = 0$ and thus, the finite-dimensional slow system takes the form

$$dx_s/dt = f_0(x_s) + \sum_{i=1}^{l} B_0^i\, a_0^i(x_s,0,\bar{v},t)$$
$$y_{cs}{}^i = C^i x_s = h^i{}_0(x_s) \quad (35)$$

For the above system, one can show (see ref 13 for details) that it is locally exponentially stable provided that assumptions 1 and 2 of the theorem hold and that the input/output response of eq 30 is enforced. Finally, since the infinite-dimensional fast subsystem of eq 34 is exponentially stable, an application of proposition 1 in ref 7 (singular perturbation stability result for infinite dimensional systems) yields that there exists an ϵ^*, such that if $\epsilon \in (0, \epsilon^*)$, $\max\{|x_s(0)|, ||x_f(0)||_2\} \le \delta$, then the state of the closed-loop parabolic PDE system of eq 31 is asymptotically stable and that its outputs satisfy the relation of eq 30.

Remark 2. We note that the controller of eq 28 uses static feedback of the measured outputs y_m^κ, $\kappa = 1, ..., p$, and thus, it feeds back both x_s and x_f. However, even though the use of x_f feedback could lead to destabilization of the stable fast subsystem, the large separation of the slow and fast modes of the spatial differential operator (i.e., ϵ is sufficiently small) and the fact that the controller does not include terms of the form $O(1/\epsilon)$ do not allow such a destabilization to occur.

Remark 3. The main benefit of static output feedback control versus dynamic (state observer-based) output feedback control[7] is the ease of on-line implementation of the controller. In particular, the static output feedback controller of eq 28 does not use a state observer (a dynamical system which has to be simulated on-line to provide estimates of the state variables from the measurements), and thus, the control action can be instantaneously computed on-line. On the other hand, it is important to note that this computational benefit comes at the expense of using a larger number of measurements (note that according to assumption 1, $p = m$: the number of sensors needed is equal to the number of slow modes) and higher sensitivity of the static output feedback controller to measurement noise.

Nonlinear Static Output Feedback Control of RTCVD

In this section, we illustrate the application of the proposed output feedback control method to the RTCVD process. Initially, an accurate solution of the model of the RTCVD process (eqs 1, 4, and 5) was computed by using a finite difference scheme with 100 discretization points. The time integration was performed by using explicit Euler, and the nonlinear boundary condition of eq 3 was solved simultaneously at each time step using a Gauss−Newton method.[23] The values of the process parameters used in our calculations are given in Table 1. A 40-s simulation run of the process with the following initial conditions, $T = 1$, $T_c = 1$, $S = 0$, $X_{SiH_4} = 0.1$, and $X_{H_2} = 0$, was used to compute 600 snapshots of the wafer temperature profile. The deviations of these snapshots from a mean spatially uniform wafer temperature profile were used as data for determining the dominant spatial temperature modes (wafer temperature empirical eigenfunctions) through Karhunen−Loéve expansion. Since we analyzed temperature profile deviations, the first eigenfunction was taken to be a spatially uniform one. We also found that the first three empirical eigenfunctions account for more than 99.0%

Table 1. Process Parameters

A_w	=	182.41×10^{-4}	m^2
A_c	=	1217.31×10^{-4}	m^2
A_{cyl}	=	794.83×10^{-4}	m^2
A_{hem}	=	422.48×10^{-4}	m^2
L_c	=	15.43×10^{-2}	m
L_s	=	10×10^{-2}	m
R_c	=	8.2×10^{-2}	m
R_w	=	7.62×10^{-2}	m
δ_z	=	0.05×10^{-2}	m
M_c	=	1422.6	$J\ K^{-1}$
q_{edge}	=	49 × 104	J s^{-1} m-2
b	=	78.95	$Torr^{-1}$
c	=	0.38	$Torr^{1/2}$
e_w	=	0.7	
e_c	=	0.37	
ρ_c	=	2.6433×10^3	kg m^{-3}
V_c	=	638.25×10^6	m^3
ρ_w	=	2.3×10^3	kg m^{-3}
$X^{in}_{SiH_4}$	=	0.1	$kmol_{SiH_4}\ kmol^{-1}_{feed}$
P_{tot}	=	5.0	Torr
MW_{Si}	=	28.086	kg $kmol^{-1}$
ρ_{Si}	=	2.3×10^3	kg m^{-3}
R	=	8.314×10^3	J $kmol^{-1}\ K^{-1}$
T_{amb}	=	300.0	K
α	=	12.961×10^6	$kmol^{-1}$
k_0	=	263.158×10^1	kmol $m^{-2}\ s^{-1}\ Torr^{-1}$
γ	=	153.809×10^6	J $kmol^{-1}$
σ	=	5.6705×10^{-8}	J $s^{-1}\ m^{-2}\ K^{-4}$
τ	=	0.380	s

of the energy contained in the ensemble of snapshots (i.e., $\lambda_2 + \lambda_3 + \lambda_4 \geq 0.99$, when $\lambda_2 + \cdots + \lambda_{\kappa+1} = 1$ where $\kappa = 600$ is the number of snapshots). Then, a collocation formulation of Galerkin's method was used to obtain a low-order model that describes the wafer temperature. The first three empirical eigenfunctions together with the spatially uniform eigenfunction were used as basis functions. The roots of the highest-order trial function were used as collocation points; thereby forcing the residual to be orthogonal, and therefore zero, at these points. Specifically, the following collocation points were used: $r = 0.35$, $r = 0.72$, and $r = 0.99$. Additional collocation points were added at $r = 0.0$ and $r = 1.0$ to satisfy the boundary conditions imposed there. This fifth-order model was used to synthesize a nonlinear multivariable *static* output feedback controller using the controller synthesis formula of theorem 1. The controller uses point measurements of the wafer temperature at the five collocation points and adjusts the powers of the four top lamps (see Figure 1 for a schematic of the control configuration) to control the wafer temperature at the following four points: $r = 0.0$, $r = 0.35$, $r = 0.72$, and $r = 0.99$. Note that four controlled outputs are considered because four manipulated inputs are used, and five measurements are assumed to be available since the dimension of the model used for controller synthesis is also five (assumption 1).

A simulation run was performed to evaluate the performance of the nonlinear controller for a 40-s cycle with initial conditions $T = 1$, $T_c = 1$, $S = 0$, $X_{SiH_4} = 0.1$, and $X_{H_2} = 0$. Figure 2 shows the spatiotemporal evolution of the wafer (a), the temperature distribution along the radius of the wafer at $t = 40$ s (b), and the thickness of the deposition (c). The profiles of the four manipulated inputs are shown in Figure 3 (note that $u_i(t)$ = (power in ith concentric region of the top lamp)/(5000 W)). The performance of the nonlinear controller is excellent, achieving an almost uniform (less that 1% variation) thin-film deposition. We also implemented on the process four proportional integral (PI) controllers with the following parameters for proportional gain: $K_{ci} = 0.65$

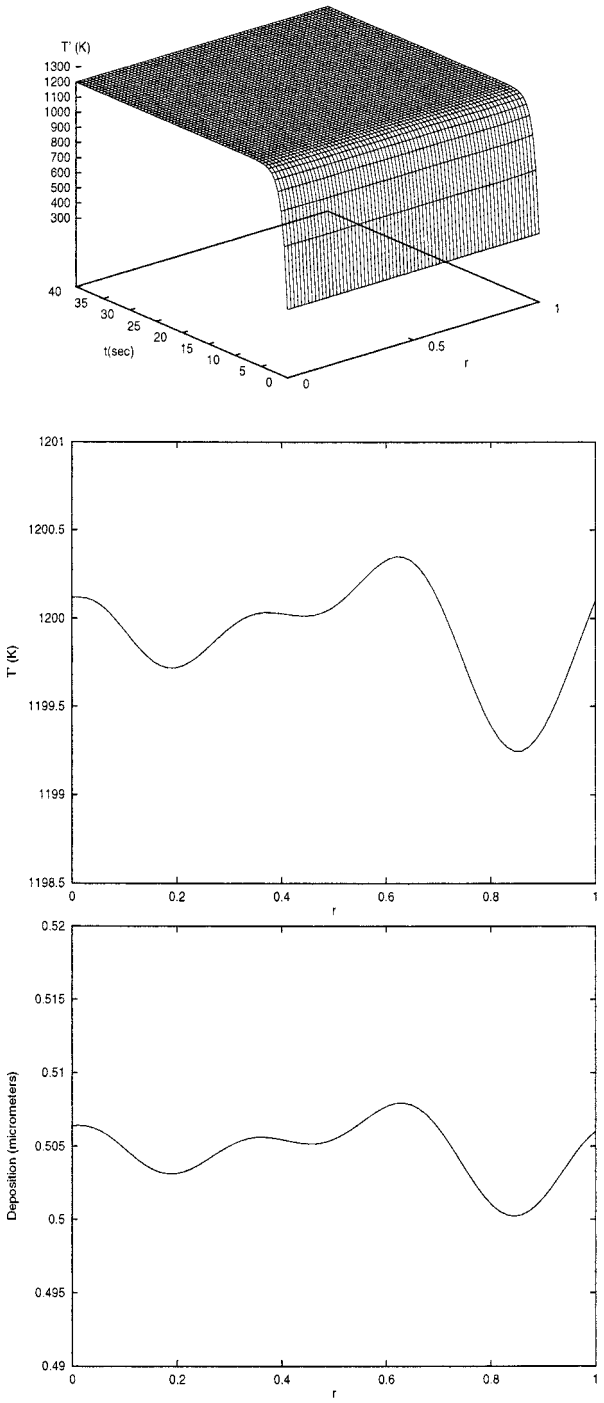

Figure 2. Closed-loop spatiotemporal wafer temperature profile (top), wafer temperature profile at $t = 40$ s (middle), and deposition thickness profile at $t = 40$ s (bottom) under nonlinear static output feedback control.

and integral time constant $\tau_{Ii} = 10.0$ for $i = 1, 2, 4, 4$ (these values were computed through extensive trial and error). The first PI controller is used to adjust the power of the first concentric lamp by using a point temperature measurement at $r = 0$, the second PI controller adjusts the power of the second concentric lamp by using a temperature measurement at $r = {}^1/_3$, the third PI controller adjusts the power of the third concentric lamp by using a temperature measurement at $r = {}^2/_3$, and the fourth PI controller adjusts the power of the fourth concentric lamp by using a temperature measurement at $r = 1$. The final film thickness at $t = 40$ s obtained under PI control is displayed in Figure 4 (dashed line)

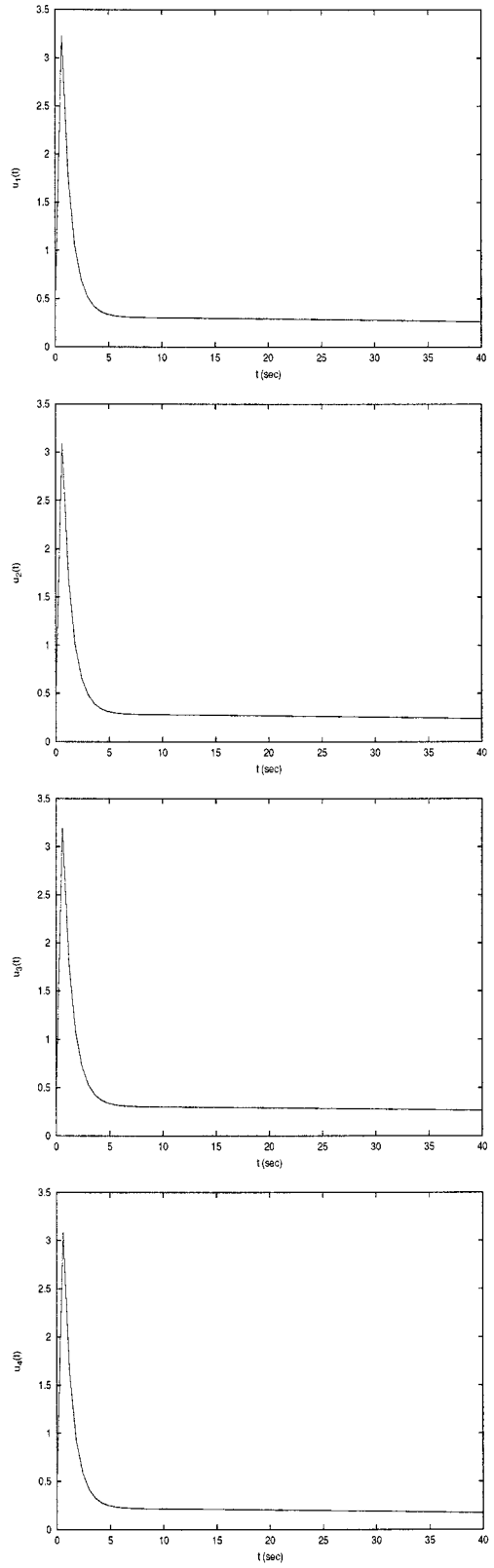

Figure 3. Manipulated input profiles for nonlinear static output feedback control.

and compared to the one achieved by the nonlinear static output feedback controller (solid line). Clearly, the performance of the four PI controllers is worst (more than 5% variation in final thin-film thickness) than the one by the nonlinear controller.

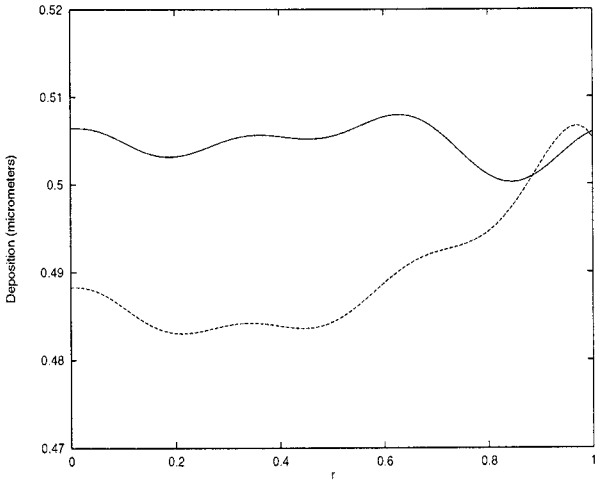

Figure 4. Deposition thickness profiles at $t = 40$ s of the closed-loop system under proportional integral control (dashed line) and nonlinear static output feedback control (solid line).

Conclusions

This work presented a general method for the synthesis of nonlinear static output feedback controllers for parabolic PDE systems with nonlinear spatial differential operators. Initially, the Karhunen−Loéve expansion was employed to derive empirical eigenfunctions of the nonlinear parabolic PDE system, then the empirical eigenfunctions were used as basis functions within a Galerkin model reduction framework to derive low-order ODE systems that accurately describe the dominant dynamics of the PDE system, and finally, these ODE systems were utilized for the synthesis of nonlinear static output feedback controllers that guarantee stability and enforce output tracking in the closed-loop system. The proposed control method was successfully employed to synthesize a nonlinear easy-to-implement controller for a RTCVD process that uses measurements of wafer temperature at five locations to manipulate the power of the top lamps in order to achieve uniform temperature and, thus, uniform deposition of a thin film on the wafer over the entire process cycle. The performance of the controller was successfully tested through simulations and was shown to be superior to the one of a linear control scheme.

Acknowledgment

Financial support for this work from a National Science Foundation CAREER award, CTS-9733509, is gratefully acknowledged.

Literature Cited

(1) Balas, M. J. Feedback control of linear diffusion processes. *Int. J. Control* **1979**, *29*, 523−533.

(2) Banerjee, S.; Cole, J. V.; Jensen, K. F. Nonlinear model reduction of rapid thermal processing systems. *IEEE Trans. Sem. Manuf.* **1998**, *11*, 266−275.

(3) Bangia, A. K.; Batcho, P. F.; Kevrekidis, I. G.; Karniadakis, G. E. Unsteady 2-D flows in complex geometries: Comparative bifurcation studies with global eigenfunction expansion. *SIAM J. Sci. Comput.* **1997**, *18*, 775−805.

(4) Breedijk, T.; Edgar, T. F.; Trachtenberg, I. A model predictive controller for multivariable temperature control in rapid thermal processing. In *Proceedings of American Control Conference*, San Francisco, CA, 1993; pp 2980−2984.

(5) Butler, S. W.; Edgar, T. F. Case studies in equipment modeling and control in the microelectronics industry. *AIChE Symp. Ser.* **1997**, *93*, 133−144.

(6) Christofides, P. D. Robust control of parabolic PDE systems. *Chem. Eng. Sci.* **1998**, *53*, 2949−2965.

(7) Christofides, P. D.; Daoutidis, P. Finite-dimensional control of parabolic PDE systems using approximate inertial manifolds. *J. Math. Anal. App.* **1997**, *216*, 398−420.

(8) Foias, C.; Jolly, M. S.; Kevrekidis, I. G.; Sell, G. R.; Titi, E. S. On the computation of inertial manifolds. *Phys. Lett. A* **1989**, *131*, 433−437.

(9) Foias, C.; Sell, G. R.; Titi, E. S. Exponential tracking and approximation of inertial manifolds for dissipative equations. *J. Dyn. Differ. Equations* **1989**, *1*, 199−244.

(10) Fukunaga, K. *Introduction to statistical pattern recognition;* Academic Press: New York, 1990.

(11) Graham, M. D.; Kevrekidis, I. G. Alternative approaches to the Karhunen−Loeve decomposition for model reduction and data analysis. *Comput. Chem. Eng.* **1996**, *20*, 495−506.

(12) Holmes, P.; Lumley, J. L.; Berkooz, G. *Turbulence, Coherent Structures, Dynamical Systems and Symmetry;* Cambridge University Press: New York, 1996.

(13) Isidori, A. *Nonlinear Control Systems: An Introduction*, 2nd ed., Springer-Verlag: Berlin-Heidelberg, 1989.

(14) Kokotovic, P. V.; Khalil, H. K.; O'Reilly, J. *Singular Perturbations in Control: Analysis and Design;* Academic Press, London, 1986.

(15) Park, H. M.; Cho, D. H. The use of the Karhunen−Loeve decomposition for the modeling of distributed parameter systems. *Chem. Eng. Sci.* **1996**, *51*, 81−98.

(16) Ray, W. H. *Advanced Process Control;* McGraw-Hill: New York, 1981.

(17) Schaper, C. D. Real-time control of rapid thermal processing. In *Proceedings of American Control Conference,* San Francisco, CA, 1993; pp 2985−2989.

(18) Shvartsman, S. Y.; Kevrekidis, I. G. Nonlinear model reduction for control of distributed parameter systems: A computer assisted study. *AIChE J.* **1998**, *44*, 1579−1595.

(19) Sirovich, L. Turbulence and the dynamics of coherent structures: part I: Coherent structures. *Q. Appl. Math.* **1987**, *45*, 561−571.

(20) Sirovich, L. Turbulence and the dynamics of coherent structures: part II: Symmetries and transformations. *Q. Appl. Math.* **1987**, *45*, 573−582.

(21) Stuber, J. D.; Edgar, T. F.; Breedijk, T. Model-based control of rapid thermal processes. In *Proceedings of the Electrochemical Society*, Reno, NV, 1995; Vol. 4, pp 113−147.

(22) Temam, R. *Infinite-Dimensional Dynamical Systems in Mechanics and Physics*; Springer-Verlag: New York, 1988.

(23) Theodoropoulou, A.; Adomaitis, R. A.; Zafiriou, E. Model reduction for optimization of rapid thermal chemical vapor deposition systems. *IEEE Trans. Sem. Manuf.* **1998**, *11*, 85−98.

(24) Theodoropoulou, A.; Adomaitis, R. A.; Zafiriou, E. Inverse model based real-time control for temperature uniformity of RTCVD. *IEEE Trans. Sem. Manuf.* **1999**, *12*, 87−100.

Received for review February 22, 1999
Revised manuscript received July 23, 1999
Accepted August 13, 1999

IE990131C